HAYATI
Journal of Biosciences

Vol. 33 No. 2, March 2026 360-370
DOI:10.4308/hjb.33.2.360-370
ISSN: 1978-3019
EISSN: 2086-4094

Research Article

Silicon Enhances Banana Resistance to *Fusarium oxysporum* f.sp. *cubense* through Ethylene Signaling Modulation and Root Tissue Protection

Arief Pambudi[1,2], Yunus Effendi[3], Lisdar I Sudirman[4], Miftahudin[4*]

[1]*Plant Biology Graduate Program, Department of Biology, Faculty of Mathematics and Natural Sciences, IPB University, Bogor 16680, Indonesia*
[2]*Biology (Biotechnology) Department, Faculty of Science and Technology, Universitas Al Azhar Indonesia, Kebayoran Baru, Jakarta 12110, Indonesia*
[3]*Graduate Program in Natural Resources Management, Faculty of Science and Technology, Universitas Al Azhar Indonesia, Kebayoran Baru, Jakarta 12110, Indonesia*
[4]*Department of Biology, Faculty Mathematics and Natural Sciences, IPB University, Bogor 16680, Indonesia*

ARTICLE INFO

Article history:
Received June 13, 2025
Received in revised form July 17, 2025
Accepted October 6, 2025
Available Online November 12, 2025

KEYWORDS:
banana,
ethylene signaling,
Fusarium wilt,
gene expression,
root anatomy,
Silicon

ABSTRACT

Fusarium oxysporum f.sp. *cubense* Tropical Race 4 (Foc TR4) is an agent of banana's vascular wilt that severely hampers production. It has been indicated that silicon (Si) might play a role in plant defense, but the banana–Foc pathosystem mechanism needs to be investigated. This study aimed to assess the impact of Si supplementation on banana plant responses to Foc infection, particularly using a completely randomized design arranged in four treatments: Control, Foc, Si, and Si*Foc. The transcript levels of the ethylene-receptor (*EIN1, EIN3*), ethylene-response factor (*ERF1, ERF2*), and the defense marker *PR4* were quantified using qRT-PCR. Phenotypic observation, corm lesion severity, and root anatomy were also evaluated. Results indicated that early ethylene signaling (*EIN1, EIN3*) was down-regulated, and *ERF2* was up-regulated in the presence of Si during Foc infection. Foc-infected plants treated with Si displayed smaller lesion areas, greater root structural stability, and less aerenchyma formation. Plant growth reduction caused by Foc was also relieved by Si, showing increased root-to-shoot biomass ratios and modified leaf shape. Multivariate analysis validated differences in physiological and transcriptional patterns in Si*Foc plants. These results indicate that Si improves banana resistance to Foc by regulating ethylene-mediated defense, tissue integrity, and stress resistance.

1. Introduction

Banana (*Musa* spp.) is a major fruit crop grown in the world's tropical and subtropical regions, providing a staple food and income to millions. However, its production is under severe threat from *Fusarium oxysporum* f.sp. *cubense* (Foc), the soil-borne fungus causing Fusarium wilt. Upon penetration of the root system by the infecting pathogen, it colonizes the vascular tissues (mainly the xylem), causing wilting, yellowing of leaves, and plant death. Though xylem occlusion is usually considered the primary determinant of disease manifestations, initial stages of infection generally occur at the epidermis and cortex, which are important penetration sites for the pathogen (Li *et al.* 2017; Zhou *et al.* 2023). Cortex tissue decay weakens the capacity of roots to form physical and chemical barriers and supports pathogen movement into the vascular system, leading to more severe disease development.

Silicon (Si) has been identified as a potential candidate for improving plant resistance to biotic stress. Although it is not deemed an essential element, Si has been demonstrated to reinforce physical barriers by deposition

* Corresponding Author
E-mail Address: miftahudin@apps.ipb.ac.id

in the cell wall and to regulate major hormonal signaling factors that play roles in plant defense (Fauteux *et al.* 2005; Wang *et al.* 2017). In bananas, Si is predominantly deposited in the epidermal cell and cortex, which may serve as a barrier to pathogen penetration in the early stages of infection. Aside from physical protection, Si has been shown to control transcriptional responses, including hormones such as ethylene, jasmonic acid, and salicylic acid.

Among them, the signaling network of ethylene is essential for regulating defense responses to both necrotrophic pathogens and wounding. Ethylene perception and signaling components include *EIN1* and *EIN3*, as well as ethylene-responsive transcription factors (ERFs), including *ERF1* and *ERF2*, which are known to mediate the expression of defense genes, like *PR4* (Müller & Munné-Bosch 2015). However, the Si-ethylene crosstalk in the process of Fusarium infection in bananas has not been well-studied. Our previous study showed that Si application in bananas up-regulated the defense-related genes, including *Allene Oxide Synthase (AOS), WRKY33* and *WRKY71* transcription factors, and genes related to energy metabolism such as ATP synthase (Pambudi *et al.* 2023). These results imply that Si rearranges molecular pathways to enhance stress resilience and maintain physiological homeostasis under pathogen attack. Similar Si-mediated enhancement of defense responses has also been reported in cucumber, where Si improved antioxidant capacity and photosynthetic performance under Fusarium infection (Sun *et al.* 2022). In addition, Si has been shown to induce systemic resistance (ISR) against other pathogens, including powdery mildew, via abiotic elicitation mechanisms (Hatem & Ali 2023), further supporting its broad-spectrum role in reinforcing plant immunity.

To further understand the role of silicon in banana resistance to Fusarium wilt, we examined its effect on ethylene-related gene expression during the early phase of Foc infection (0 and 7 days post-infection). These molecular changes were then related to long-term anatomical responses, such as corm lesion development and aerenchyma formation, observed 12 months after infection. This study specifically aimed to determine how Si modulates ethylene signaling in the early stages of Foc infection and how these molecular responses are linked to structural defense mechanisms in banana.

2. Materials and Methods

2.1. Research Design

This study was carried out at several facilities of the Department of Biology, IPB University, comprising the Plant Physiology and Genetics, Mycology, Integrated Laboratories, and the greenhouse. The plant material was a five-month-old Cavendish S99 (AAA) line banana shoot derived from tissue culture (SEAMEO BIOTROP). The *Fusarium oxysporum* f. sp. *cubense* Tropical Race 4 (Foc TR4) isolate (accession no. F822/Indo8) was acquired from InaCC, BRIN (Maryani *et al.* 2019).

A completely randomized design was used with four treatments (Control, Foc, Si, and Si*Foc) and 10 replications for each treatment. Transferred shoots were cultivated in 20 × 20 cm polybags filled with 5 kg of sterile soil:compost: burnt rice husks (3:1:1, v/v) and allowed to acclimatize for 14 days. Si in 1.6 mM concentration was applied by foliar spray and root drenching with BioSilac™ (PPKS Bogor, Indonesia), a liquid Si fertilizer containing orthosilicic acid.

Foc TR4 was cultured in PDA for 7 days and then subcultured in ¼ PDB for 5 days. Conidiospores were collected by filtration, enumerated using a hemacytometer, and adjusted to 1×10^5 conidiospores/mL (Putri *et al.* 2023) in sterile water. Inoculation occurred 14 days after Si treatment when 100 mL of the suspension was poured around the roots after wounding. Control plants were treated with 100 mL of sterile distilled water following the same root-wounding techniques.

2.2. RNA Extraction and cDNA Synthesis

RNA was extracted from roots at 0 and 7 dpi by an organic extraction method modified by Pambudi *et al.* (2023). About 2–5 g of tissue was ground into powder in liquid nitrogen and extracted with 8 mL of RNase-free buffer (3% CTAB, 2% PVP, 2 M NaCl, 20 mM EDTA, 100 mM Tris-HCl, pH 8, 2% β-mercaptoethanol). The lysate was purified by chloroform (0.6× volume) and precipitated in cold isopropanol. The RNA pellet was air-dried for 3 min, then dissolved in 1 mL of nuclease-free water (NFW). Then, 800 µL GENEzol™ reagent (Geneaid®, Taiwan) was added, and additional purification was carried out according to the manufacturer's instructions. The RNA precipitate

was dissolved in 100–200 µL of NFW and quantified on a MaestroNano™ spectrophotometer (Maestrogen®, Taiwan).

Synthesis of cDNA was carried out using one µg total RNA and the ReverTra Ace™ qPCR RT Master Mix with gDNA Remover (Toyobo®, Japan), in which a mixture of random hexamer and oligo(dT) primers was used. The manufacturer's instructions set up the reaction and conditions for thermal cycling. Each cDNA sample was diluted to a working concentration of 50 ng/µL using NFW and re-quantified to ensure consistency in gene expression analysis.

2.3. Quantitative Gene Expression Analysis

The expression of five ethylene signaling and defense-related genes (Table 1) was examined using a QuantStudio™ 5 RT-qPCR System (Applied Biosystems®, USA). All reactions were made in three biological and two technical replications, employing the SensiFAST™ SYBR Lo-Rox kit (Bioline®, UK). The 10 µL reaction consisted of 50 ng cDNA, 0.5 µM of each primer, and 1× master mix. The thermal program for the amplification was 95°C for 2 min (initial denaturation), 95°C for 10 s, 60°C for 30 s (annealing), and 72°C for 30 s (extension) during 50 cycles. Specific amplification was confirmed by melting curve analysis. Ct values were taken at the extension step, and gene expression was determined by $2^{-\Delta\Delta Ct}$ (Livak & Schmittgen 2001) and normalized to the ACT. The standard error (SE) was derived from these expression values for each treatment. The change in gene expression at day 7 relative to day 0 was calculated as: Percentage (%) = (Expression at 7 dpi – Expression at 0 dpi) / Expression at 0 dpi × 100. The change of gene expression results was visualized using a heatmap.

2.4. Morphological Observation

Morphological growth was measured during 65 days. The parameters quantified were shoot height increment, length and width of the leaves, the leaf length-to-width ratio, fresh and dry weight of the portion of shoot and root, and the root-to-shoot weight ratio. Leaf dimensions were measured with ImageJ. Chlorophyll content was estimated from leaf greenness using a SPAD chlorophyll meter (SPAD-520Plus™, Konica Minolta®, Japan), and readings were done on all the replications from every leaf.

2.5. Corm Tissue Lesion Assessment

Lesion analysis was conducted on 12-month-old infected plants to confirm infection-induced damage. The central corm was designated Generation-0 (G0), and the emerging daughter corms were Generation-1 (G1). Both G0 and G1 corms were assessed. After soil removal, each cleaned corm was horizontally sliced into uniform cross-sections, photographed, and analyzed using ImageJ. The lesion area was quantified as the percentage of the total cross-sectional area. Mean lesion percentages were calculated for each treatment.

2.6. Root Morphology and Aerenchyma Evaluation

Root morphology and anatomy of 12-month-old plants post-infection were studied. After uprooting, the roots were preserved in 70% ethanol until observation. For morphological observation, the preserved root was soaked for 1 hour with distilled water, then stained with 1% (w/v) safranin) for 10 min and examined under a digital stereo microscope (Edge Plus™ AM8917, Dino Lite®, Indonesia).

Table 1. List of genes analyzed in this research

Gene name	Biological function	Primers	Sequences	Amplicon size (bp)
Ethylene insensitive 1	Ethylene receptor	*EIN1-F*	5'-AAACCCAATTCAGGCCAC-3'	412
		EIN1-R	5'-AAGATGTCTCGTGCACAGGA-3'	
Ethylene insensitive 3	Ethylene receptor	*EIN3-F*	5'-GCATAGTGGGAGAGGGAGAC-3'	374
		EIN3-R	5'-CCTTCTCCTTCCACCAACC-3'	
Ethylene response factor 1	Ethylene effector	*ERF1-F*	5'-TGCCCATGATCAGCTTCG-3'	454
		ERF1-R	5'-CCTCGCCTCCTTCTTGATCT-3'	
Ethylene response factor 2	Ethylene effector	*ERF2-F*	5'-CCTCGACAGGGTGGAGGAG-3'	391
		ERF2-R	5'-GCCTCCCTCTTCCTTTTCC-3'	
Pathogenesis related 4	Chitinase binding	*PR4-F*	5'-GCCACGAAGAAGAGGGAG-3'	431
		PR4-R	5'-GGTCTGGGTTGTTGAGGAG-3'	
β-Actin (internal control)	Housekeeping	*ACT-F*	5'-GCCAGTGGTCGTACAACCG-3'	218
		ACT-R	5'-TCATGAGGTAATCAGTAAGGTCAC-3'	

Anatomical examination focused on the maturation zone of the root (1–2 cm from the root tip). The preserved roots were cut at 15 µm thickness with a GSL1 sliding microtome (WSL, Switzerland), stained with 1% (w/v) safranin for 1 min, washed, and mounted in 30% (v/v) glycerol. The root sections were observed using an Olympus® CX33 light microscope (Japan) with an Indomicro® XCAM-1080PHA camera (Indonesia) at 40× magnification. The image analysis of the aerenchyma and the measurement of the total root cross-section area were performed using ImageJ. The aerenchyma area was calculated as a percentage of the total root cross-sectional area (Hidayati *et al.* 2018). Average values for each treatment were determined.

2.7. Statistical Analysis and Data Visualization

Data for each parameter were averaged per treatment and analyzed for statistical significance using one-way ANOVA in MS Excel with the Data Analysis Toolpak VBA add-in. When significant differences were detected, Tukey's post hoc test was applied at $\alpha = 0.05$. Multivariate analyses such as PCA, heatmap, and Bi-plot were conducted using R Studio (v4.4.1) and Orange Data Mining (v3.37.0).

3. Results

3.1. Expression of Ethylene-Related Genes is Induced by Fusarium Infection and Modulated by Silicon Application

At 0 dpi (14 days after silicon supplementation), the expression of *EIN1* was markedly reduced in Si-treated plants, indicating early suppression of ethylene perception even before pathogen challenge. A similar downregulation pattern was observed for *ERF1* and *PR4*, suggesting that these genes are tightly regulated by upstream ethylene signaling and that silicon may attenuate baseline defense gene expression under non-stress conditions. In contrast, *ERF2* maintained a relatively basal expression level across all treatments at this stage.

By 7 dpi, infection and treatment interactions led to strikingly different gene expression profiles, as visualized in the heatmap (Figure 1F). *ERF2* showed a sharp induction across all treatments compared to day 0, with the highest expression observed under Foc-only treatment. This pattern suggests that *ERF2* is strongly responsive to pathogen presence, potentially through signaling routes that operate independently of the *EIN1–EIN3* cascade. Notably, *EIN3*—though reduced over time—was significantly upregulated under the combined Si*Foc treatment at 7 dpi. This implies that EIN3 is inducible under co-stress conditions, possibly as a primed regulatory response facilitated by Si.

Meanwhile, *EIN1* and *ERF1* remained consistently low under Si-containing treatments, indicating sustained suppression of upstream ethylene signaling. Interestingly, *PR4* expression declined further after infection, especially in Si-treated roots, and did not follow the induction trend of *ERF2*. This suggests that *PR4* activation requires a fully functional upstream ethylene pathway, dampened by Si supplementation. Altogether, these findings highlight the nuanced regulatory effects of Si, which suppresses early ethylene signaling while selectively enabling the activation of key downstream genes such as *EIN3* and *ERF2* during infection.

3.2. Silicon Modulates Plant Growth and Biomass under Fusarium Stress

Foc infection inhibited plant growth and biomass accumulation, effects that were only partially mitigated by silicon supplementation (Tables 2–4). Plant height was significantly reduced in Foc-infected plants compared to the control, confirming the pathogen's negative impact on vegetative growth. Si treatment alone moderately promoted height gain, possibly by enhancing physiological stability or nutrient efficiency. Under the Si*Foc treatment, height remained suppressed but showed slight improvement compared to Foc alone. This partial recovery suggests that while Si alleviates early infection stress, it cannot fully restore normal growth. It is likely due to a defense–growth trade-off, in which energy is redirected from elongation to stress adaptation.

Leaf morphology also changed under stress. Leaf length and width significantly decreased in Foc and Si*Foc treatments, with the narrowest leaves observed in the Si*Foc group (Table 2). Interestingly, the length-to-width ratio increased under both treatments, indicating a stress-related shift in leaf shape. Chlorophyll content showed no statistically significant differences, although a decreasing trend was observed in all Foc-infected groups, with or without silicon.

Biomass data followed similar trends. Foc infection reduced fresh and dry biomass, particularly in shoot and total plant weight (Tables 3 and 4), mirroring reductions in plant height and leaf size. Differences were not statistically significant, probably because of limited sample replication. Notably, Si supplementations

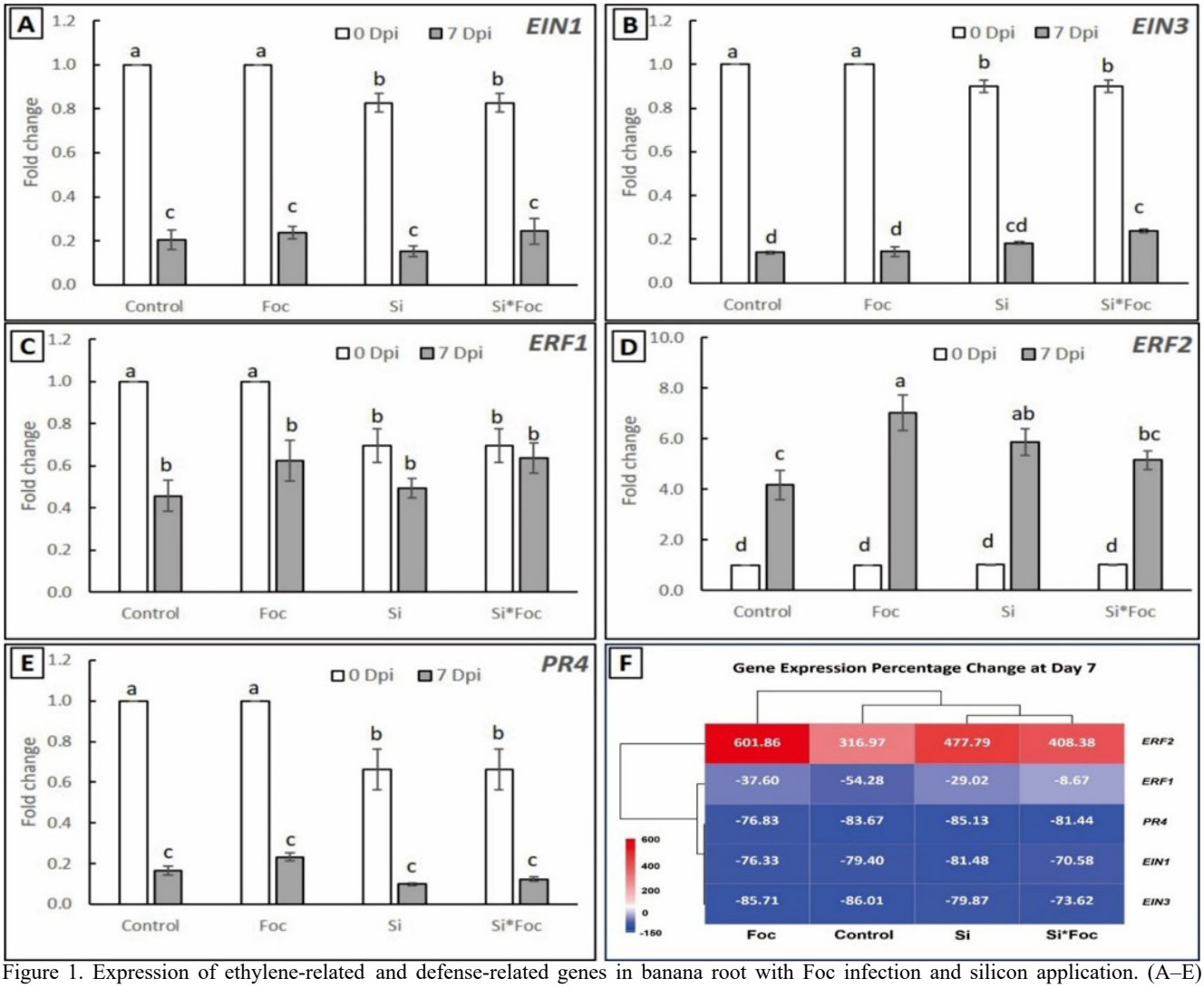

Figure 1. Expression of ethylene-related and defense-related genes in banana root with Foc infection and silicon application. (A–E) Relative expression of *EIN1, EIN3, ERF1, ERF2*, and *PR4* genes was measured by qRT-PCR at 0 dpi (14 days after Si supplementation) and 7 dpi for Control, Foc, Si, and Si*Foc treatments. The different letters showed a significant level with Tukey's HSD ($p<0.05$). (F) Heatmap showing the percentage change in gene expression at 7 dpi relative to 0 dpi. The heatmap highlights a marked induction of *ERF2*, particularly under Foc infection only, and general repression of *EIN1/3, ERF1*, and *PR4* under Si-containing treatments. All gene expression was normalized to the internal control gene (*ACT*). Gene abbreviation *EIN1: Ethylene Insensitive1, EIN3: Ethylene Insensitive3, ERF1: Ethylene Response Factor 1, ERF2: Ethylene Response Factor 2*, *PR4: Pathogenesis Related 4, ACT: β-Actin*

tended to increase shoot and root fresh weights, indicating partial physiological recovery.

The morphological changes are also visible in representative plant photographs for each treatment group (Figure 2). Foc-infected plants are smaller and have narrower leaves than control and Si-treated plants. Generally, Si mitigated some of the negative effects of Foc infection on growth and biomass, but it was insufficient to restore growth to the control levels fully.

3.3. Silicon Mitigates Root Lesion Severity and Inhibition of Aerenchyma Formation upon Fusarium Infection

Following the analysis of changes in gene expression, which revealed silicon-responsive expression in ethylene signaling and defense-related genes, morphological and anatomical changes in banana root tissues were investigated to confirm the effect of Si supplementation. Banana corm showed visible tissue damage upon infection with Foc, observed by the

Table 2. Plant growth parameters under various treatments

Treatment	Height growth, HG (%)	Leaf length, LL (cm)	Leaf width, LW (cm)	Leaf length:widht ratio, (LWR)	Chlorophyll (SPAD unit)
Control	47.35±2.80[a]	28.61±1.17[a]	15.35±0.68[a]	1.90±0.06[b]	45.28±1.16[a]
Foc	27.25±4.08[b]	27.02±1.01[a]	13.70±0.68[ab]	2.05±0.07[ab]	42.22±0.79[a]
Si	37.01±4.01[ab]	25.33±0.74[a]	13.54±0.48[ab]	1.91±0.06[ab]	45.11±0.42[a]
Si*Foc	26.01±4.93[b]	25.50±0.78[a]	12.00±0.44[b]	2.16±0.05[a]	42.72±1.57[a]

The data show the mean ± Standard Error (SE) with sample number (n) varying between each variable (HG: 10, LL: 30, LW: 30, LWR: 30, Chlorophyll: 10). Different letters in each column indicate significance values based on Tukey's HSD test ($p<0.05$)

Table 3. Fresh biomass of banana plants under different treatments

Treatment	Fresh shoot weight, FS (g)	Fresh root weight, FR (g)	Total fresh weight, TF (g)	Fresh root: shoot ratio (FRSR)
Control	105.13±31.44	138.51±3.56	243.64±27.88	1.46±0.47
Foc	68.35±17.28	118.01±18.35	186.35±35.62	1.77±0.18
Si	99.81±3.94	171.7±18.71	271.51±22.65	1.72±0.12
Si*Foc	71.95±1.65	141.6±8.58	213.55±6.93	1.97±0.16

The data show the mean ± Standard Error (SE) with sample number (n) varying between each variable (FS: 2, FR: 2, TF: 2, FRSR: 2). All treatments did not significantly affect fresh biomass and root: shoot ratio

Table 4. Dry biomass of banana plants under different treatments

Treatment	Dry shoot weight, DS (g)	Dry root weight, DR (g)	Total dry weight, TD (g)	Dry Root: shoot ratio (DRSR)
Control	105.13±31.44	138.51±3.56	243.64±27.88	1.43±0.14
Foc	68.35±17.28	118.01±18.35	186.35±35.62	2.07±0.44
Si	99.81±3.94	171.7±18.71	271.51±22.65	1.81±0.15
Si*Foc	71.95±1.65	141.6±8.58	213.55±6.93	2.13±0.24

The data show the mean ± Standard Error (SE) with sample number (n) varying between each variable (DS: 2, DR: 2, TD: 2, DRSR: 2). All treatments did not significantly affect the dry biomass and root: shoot ratio

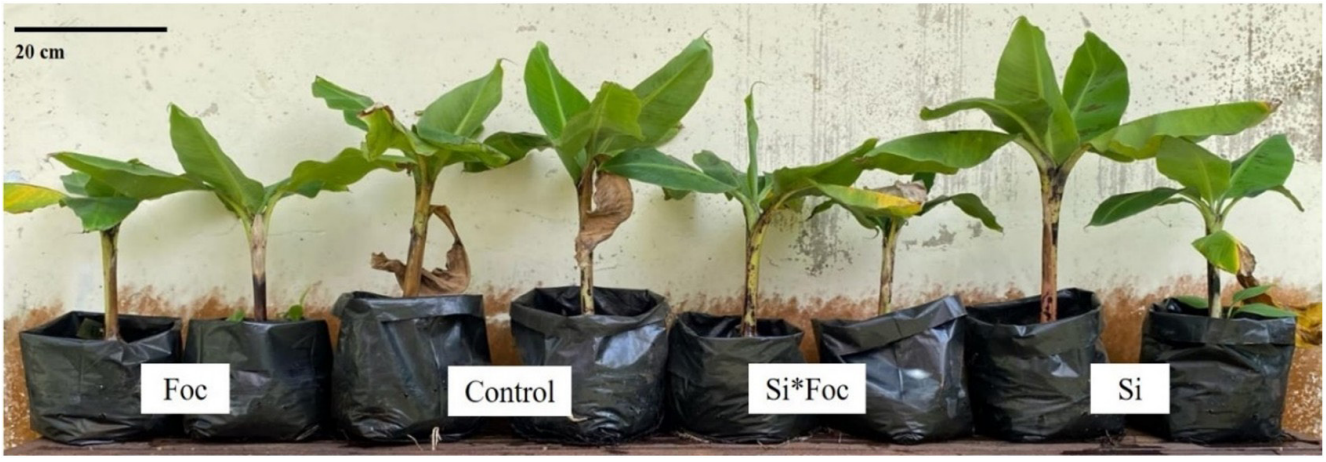

Figure 2. Banana plants harvest sample representative in each treatment: Foc, Control, Si*Foc, Si. Plant size between Foc infection and silicon supplement treatments reflected visual differences in plant height and leaf size. The plant's vigor is consistent with quantitative data in Tables 2–4, showing that growth decreased under Foc infection and partially recovered with silicon treatment

large necrotic area (Figure 3A, red arrows). However, silicon application remarkably decreased the severity of the lesions in Foc-infected plants. In contrast, the necrotic areas were significantly reduced in the Si*Foc treatment compared to the Foc treatment alone.

Aerenchyma formation in Foc-infected roots was observed by the histological analysis of root cross-sections (Figure 3B), indicating a stress response. In non-infected (control and Si-treated) roots, the cortex appeared normal, with only a small intercellular space and aerencyma. Interestingly, the silicon supplementation inhibited aerenchyma formation in the tissues of Foc-infected plants with intact anatomical structure and a dense cortex.

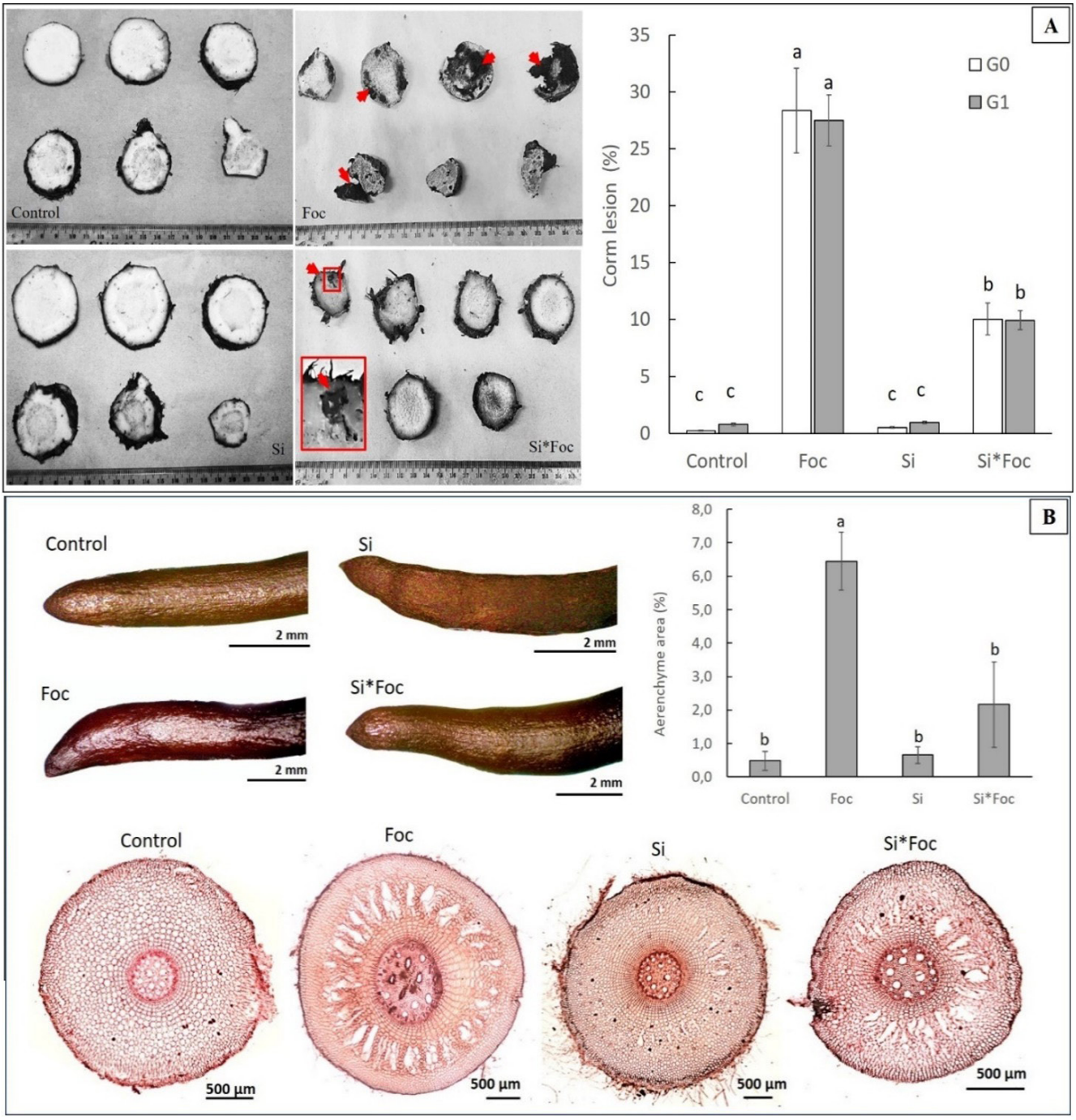

Figure 3. Effects of Si on root tissues of banana in responding to damage and aerenchyma formation when infected by Foc. (A) Corm transverse sections display necrotic lesions (red arrows) of Foc-infected plants and lesion quantification between generations (G0 and G1) in each treatment, (B) root morphology, anatomical cross-section, and quantification of aerenchyma area. Significant aerenchyma formation, as well as disrupted cortical structure, could be observed in Foc-infected roots. On the other hand, Si*Foc treatment kept cortical disruption at low levels, promoting suppressed aerenchyma formation. Bars are means ± SE, with sample number (n) varying between each variable (corm lesion n=20, aerenchyma n=4). Different letters above bars showed significant differences between treatments (Tukey's HSD test, $p<0.05$)

These anatomical data are then also confirmed by quantitative examination. The percentage of corm lesion area was substantially increased during Foc infection in primary corms (G0) and daughter corms (G1), reaching an average of almost 30% (Figure 3A, right panel). By contrast, Si treatment of plants before Foc infection (Si*Foc) resulted in much lower average lesion severity scores of approximately 10% in the two generations.

The same pattern was observed in the formation of aerenchyma. Foc infection led to a significant elevation of aerenchyma area (6.45%), which was attenuated by Si*Foc treatment and almost reached the aerenchyma percentage of 2.17% observed in the control group (Figure 3B, right panel). These results indicate that the resistance of root tissue of silicon-treated plants was increased by less necrotic extension and fewer aerenchyma formation in response to Foc infection.

3.4. Multivariate Analysis Demonstrates that Silicon Has Coordinated Effects on Growth and Stress Response in Banana

To gain an integrative perspective of plant responses in Foc infection and Si treatment, a multivariate analysis based on principal component (PCA) and hierarchical clustering was carried out. A PCA score plot (Figure 4A) demonstrates a lateral spread for treatment groups according to time (0 and 7 dpi) and stress status based

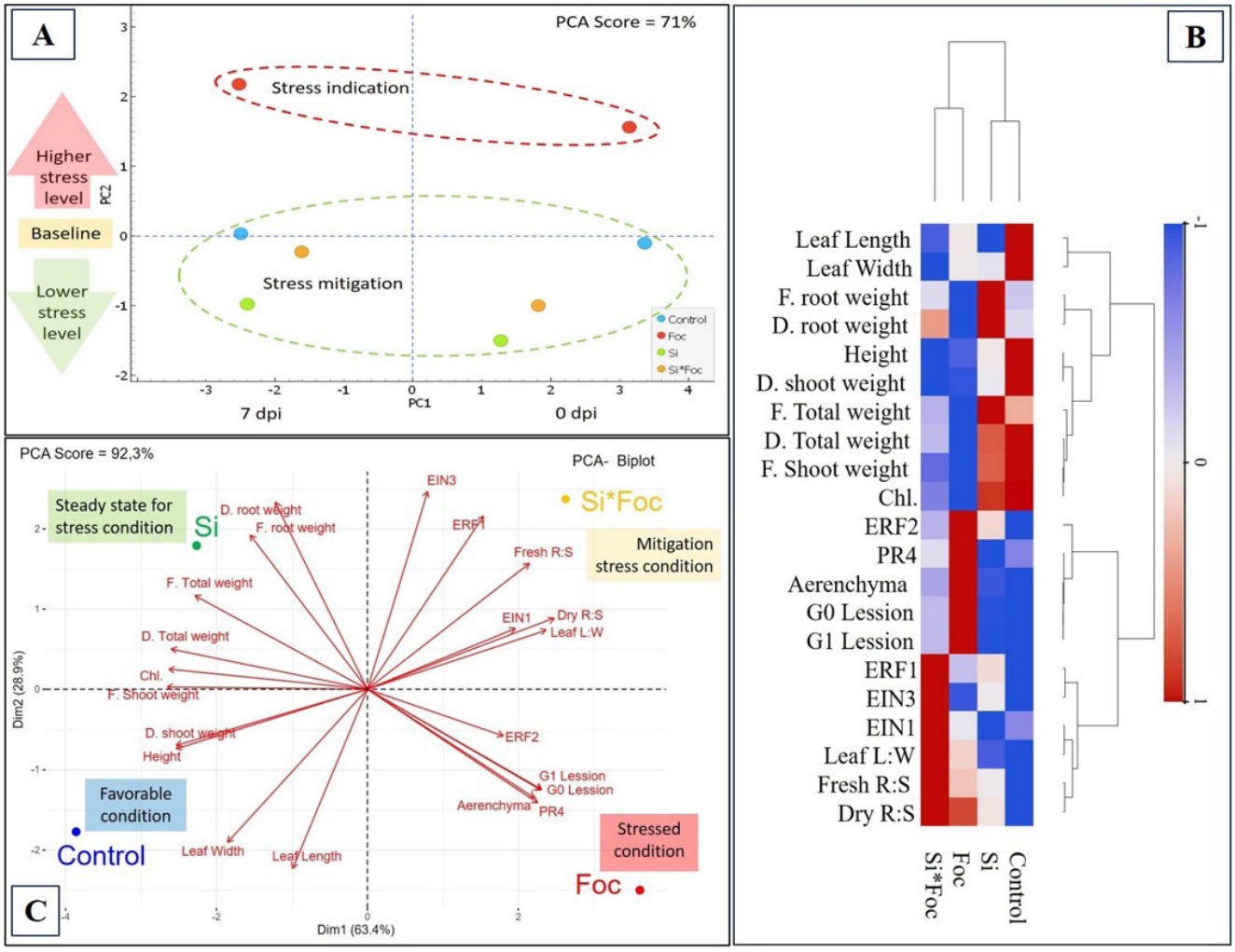

Figure 4. Multivariate analysis combining phenotypic, anatomical, and molecular variables under Foc infection and Si treatment. (A) Principal component analysis (PCA) score plot based on the expression profiles of ethylene-related and defense-related genes. The samples were grouped by treatment and time-point (0 and 7 dpi), with Foc-infected plants categorized towards the stress cluster (indicating stress) and Si*Foc grouped into the more stress-alleviated cluster (mitigating stress), (B) heatmap with hierarchical clustering of all variables, morphological traits, anatomical measurements, and gene expression. Red indicates higher values, and blue indicates lower values, (C) the PCA biplot uses all parameters to depict relationships between treatments. The Foc treatment was positively related to the degree of lesion development, aerenchyma formation, and expression of PR4 genes, suggesting stress responses. However, Si*Foc caused an increase in the root-to-shoot ratio and leaf length-to-width ratio, as well as the regulation of some ethylene signaling genes, suggesting that this variety of Si-mediated adaptive response to Foc stress

on gene expression profile. The Foc treatments are grouped independently in the upper value of PC2 to express the maximum stress caused by the measured parameters. Si treatments, however, were found to have a lower value of PC2, implying mitigation of stress and being close to the control.

Heatmap data and hierarchical clustering suggested the presence of all observed variables (Figure 4B). Genes related to ethylene perception (*EIN1, EIN3, ERF1, ERF2*), defense (*PR4*), and anatomy markers (aerenchyma and lesion formation in G0 and G1 corm tissues) were highly correlated with Foc stress. In contrast, growth-related traits (leaf length, shoot, and root weights) were mainly grouped with the control and Si-treated groups, indicating favorable conditions. APCA-biplot was also used to interpret the contributions of variables to treatment separation in different quadrants (Figure 4C). The Foc treatment highly correlates with lesion severity (G0, G1), aerenchyma development, and induction of *PR4* and *ERF2* genes, supporting its connection with a stressed phenotype. Instead, the Si*Foc treatment loaded close to growth-based variables (total plant weight, shoot height) and chlorophyll content, indicating a more beneficial physiological status under stress. Interestingly, Si alone was the closest to the center of the PCA axis, implying that it was in a stable state under stress. Generally, the multivariate analysis verified that silicon supplementation not only mitigates the damage of Foc infection but also enhances the growth of plants and influences the expression of stress-related genes.

4. Discussion

The expression profiling of ethylene-related genes in banana roots reveals a selective and temporary hormone-mediated defense response against Foc, modulated by Si. Notably, the strong upregulation of *ERF2* at 7 dpi—especially under Foc infection—suggests its role as a key downstream effector in ethylene-induced defense (Figure 1D). As part of the ethylene-responsive transcription factor family, *ERF2* is known to regulate defense-related gene networks, including certain pathogenesis-related (PR) genes (Xu *et al.* 2006; Wu *et al.* 2022), and has been implicated in resistance to hemibiotrophic pathogens such as Foc (Coskun *et al.* 2018). Interestingly, the moderate induction of *ERF2* under Si and Si*Foc treatments may reflect a primed state, where transcriptional responsiveness is enhanced without constitutive activation, allowing the plant to prepare for future stress without incurring fitness costs. In contrast, the repression of *EIN1* and *EIN3* in both Foc and Si*Foc treatments suggests inhibition of early ethylene signaling (Figure 1A and B). As positive regulators, their repression may represent a negative feedback mechanism to prevent overactivation of defense pathways that could otherwise impair growth (Ju & Chang 2015). This pattern was consistent with heatmap analysis (Figure 1F), showing the suppression of these upstream components across treatments. It suggests that Si-mediated modulation acts not only at the downstream transcription factor level but also through selective regulation of early signaling nodes, possibly to fine-tune the balance between defense activation and growth maintenance.

A notable observation was the non-parallel expression pattern between *ERF2* and *PR4*. While *ERF2* was clearly upregulated upon Foc infection, *PR4* remained consistently low and even declined further in Si-related treatments (Figure 1E). This indicates that *PR4* expression is not strictly co-regulated with *ERF2*, challenging the assumption of a linear *EIN–ERF–PR* cascade. Previous studies have shown that ethylene responses can bifurcate into multiple signaling arms, and *PR4* induction may also depend on cross-talk with jasmonic acid (JA), salicylic acid (SA), or even reactive oxygen species (ROS) pathways (Broekaert *et al.* 2006; Pieterse *et al.* 2014). Thus, while *ERF2* may reflect a specific ethylene-JA–JA synergy, *PR4* expression likely requires additional or alternative signals for activation.

In line with this, although our dataset did not directly include markers of SA or JA pathways, prior transcriptomic analysis using the same pathosystem demonstrated induction of AOS, a key gene in JA biosynthesis, upon Si application (Pambudi *et al.* 2023). This supports the idea that Si-triggered resistance involves broader hormonal crosstalk, and ethylene signaling alone may not fully explain downstream defense gene regulation. This complexity aligns with emerging perspectives that Si acts as a modulator of plant immune networks, rather than as a simple activator of single hormone pathways (Fauteux *et al.* 2005; Ahammed & Yang 2021).

Taken together, these findings suggest that Si selectively modulates ethylene signaling in banana roots under Foc infection, by enhancing downstream effectors like *ERF2* while repressing upstream *EIN1/3*, and that the activation of classical PR genes like *PR4* may involve more intricate hormonal integration. This

fine-tuned response allows the plant to manage defense signaling while minimizing energy trade-offs that could compromise growth.

The detection of corm lesions showed extensive tissue degradation under Foc infection, which was proven by blackening necrotic tissue. These symptoms were decreased in plants treated with Si (Figure 3A and C). This confirmed previous studies demonstrating that Si effectively diminishes banana Foc colonization and necrotic tissue (Fortunato *et al.* 2015; Verma *et al.* 2024). In addition, aerenchyma formation in the cortex could be due to ethylene-promoted ROS accumulation, which activates lysigenous cell death under hypoxia due to reduced oxygen concentration due to vascular blockage by Foc. The blackened corm tissue is presumed to indicate the colonization zone by Foc, whereas Si treatment reduces such spread, implying a structural and biochemical reinforcement of defense.

Consistent with this, histological analysis also supported the protective role of Si. Vascular disintegration and more aerenchyma were formed when the plants were infected by Foc, which reflects tissue stress and hypoxia. In Si*Foc plants, Foc colonization eventually retarded. Hence, the aerenchyma area decreases in the roots of Si*Foc plants (Figure 3B). Increased Si-supplemented tissue strength might be caused by lignification or callose deposition (Liang *et al.* 2015; Etesami & Jeong 2018). The high percentage of aerenchyma occurrence under Foc might be attributed to pathogen-mediated damage and the host-plant strategy to maintain gas exchange under stress (van Dongen and Licausi 2015). The repression of aerenchyma formation in Si-supplemented plants indicates better oxygen homeostasis and lower tissue decay, thereby offering again the possibility of its involvement in structural defense.

Phenotypically, applying Si reduced Foc-induced inhibitions on plant growth (Tables 2-4). Si alone did not increase shoot height or leaf length, but it preserved these parameters relative to Foc-inoculated plants, indicating its role as a modifier for protective physiological status. Consistent responses of leaf width and SPAD values to Foc and Si*Foc treatments suggest that leaves are affected by this stress and that Si partly mitigated the effect on leaf development and chlorophyll content (Luyckx *et al.* 2017; Etesami & JeongW 2018).

The enhanced leaf length: width ratio and root: shoot biomass ratio in Si*Foc-treated plants indicate an adaptive morphological response. These changes indicate a preference for root growth and long leaves to keep water and nutrient absorption under pressure, a finding reported in other species (Ma *et al.* 2011; Hou *et al.* 2023). The greater root biomass in Si-treated plants, particularly under Foc, provides evidence to support the premise that Si contributes to maintaining root growth during infection (Fortunato *et al.* 2015).

Even though Si*Foc treatment could not fully recover any of the affected total biomass back to the control level, the maintained dry root weight and manipulation of resource allocation point to a strategic physiological response. This is in line with the results of the beneficial effects reported after the application of Si, partially due to structural fortification, antioxidant buffering, and/or hormone control, thereby enabling improved growth-defense balance (van Bockhaven *et al.* 2012; Peng *et al.* 2023).

Multivariate analysis, including physiological and transcriptional variables, defined an apparent clustering of Si*Foc samples (Figure 4). Increased root-to-shoot and leaf length-to-width ratios were positively associated with Si application, suggesting a systemic adjustment to co-occurring biotic and abiotic constraints (Rodrigues *et al.* 2015). Furthermore, the dynamic pattern of gene expression (down-regulation at early infection (0 dpi) gradually restored to control levels at 7 dpi of the ethylene-related genes follows the idea that Si mediates priming, allowing for a delayed and stronger onset of defense responses (Fauteux *et al.* 2005).

The present study illustrates that the Si application enhanced banana resistance to Foc by regulating gene expression, anatomical integrity, and resource allocation. Si functions via biochemical and structural means to restrict pathogen proliferation and sustain plant growth under stress. However, more research will be required to unravel the interaction of ethylene and other phytohormones like jasmonic acid and salicylic acid in response to Si. Furthermore, the spatial determination of Si in plant tissue and transcriptomics by RNA-seq will be essential for a comprehensive understanding of regulatory networks in Si-mediated defense in banana–Foc pathosystems.

Acknowledgements

The author would like to express his gratitude to Dr. Rhomi Ardiansyah (SEAMEO BIOTROP) for the banana plant materials, Dr. Nani Maryani (Sultan Ageng

Tirtayasa University) for the TR4 isolate, and Prof. Triadiati (IPB University) for the technical assistance on the root anatomical observations. This work was supported by the Ministry of Research, Technology, and Higher Education through the research grant for the dissertation under the grant entitled "Transcriptomics analysis of the role of Silicon in the interaction between banana and *Fusarium oxysporum* f.sp. *cubense* (Foc)".

References

Ahammed, G.J., Yang, Y., 2021. Mechanisms of silicon-induced fungal disease resistance in plants. *Plant Physiol. Biochem.* 165, 200-206. https://doi.org/10.1016/j.plaphy.2021.05.031

Broekaert, W.F., Delauré, S.L., De Bolle, M.F., Cammue, B.P., 2006. The role of ethylene in host-pathogen interactions. *Annu. Rev. Phytopathol.* 44, 393-416. https://doi.org/10.1146/annurev.phyto.44.070505. 143440

Coskun, D., Deshmukh, R., Sonah, H., Menzies, J.G., Reynolds, O., Ma, J.F., Kronzucker, H.J., Belanger, R.R., 2018. The controversies of silicon's role in plant biology. *New Phytol.* 221, 1-19. https://doi.org/10.1111/nph.15343

Etesami, H., Jeong, B.R., 2018. Silicon (Si): review and future prospects on the action mechanisms in alleviating biotic and abiotic stresses in plants. *Ecotoxicol. Environ. Safety.* 147, 881-896. https://doi.org/10.1016/j.ecoenv.2017.09.063

Fauteux, F., Rémus-Borel, W., Menzies, J.G., Bélanger, R.R., 2005. Silicon and plant disease resistance against pathogenic fungi. *FEMS Microbiol. Let*. 249, 1–6.

Fortunato, A.A., Rodrigues, F.A., Nascimento, K.J.T., Kobayashi, A.K., 2015. Silicon suppresses Fusarium wilt development in banana plants. *J. Phytopathol.* 163, 743–750. https://doi.org/10.1111/jph.12303.

Hatem, M.W., Ali, H.A., 2023. Methods of inducing systemic resistance in plants by using abiotic agents to control powdery mildew pathogens. *IOP Conf. Ser.: Earth and Environmental Science*. 1252, 012004. https://doi.org/10.1088/1755 1315/1252/1/012004

Hidayati, N., Triadiati, T., Anas, I., 2018. Rooting system of rice cultivated under system of rice intensification (SRI) method which improving rice yield. *Hayati J. Biosci.* 25, 63-69. https://doi.org/10.4308/hjb.25.2.63

Hou, L., Ji, S., Zhang, Y., Wu, X., Zhang, L., Liu, P., 2023. The mechanism of silicon on alleviating cadmium toxicity in plants: a review. *Front. Plant Sci.* 14, 1141138. https://doi.org/10.3389/fpls.2023.1141138

Ju, C., Chang, C., 2015. Mechanistic insights in ethylene perception and signal transduction. *Plant Physiol.* 169, 85-95. https://doi.org/10.1104/pp.15.00845

Li, C., Yang, J., Li, W., Sun, J., Peng, M., 2017. Direct root penetration and rhizome vascular colonization by *Fusarium oxysporum* f. sp. *cubense* are the key steps in the successful infection of Brazil cavendish. *Plant Dis.* 101, 12, 2073-2078.

Liang, Y., Nikolic, M., Bélanger, R., Gong, H., Song, A., 2015. *Silicon in Agriculture: From Theory to Practice.* Springer, Cham.

Livak, K.J., Schmittgen, T.D., 2001. Analysis of relative gene expression data using real-time quantitative PCR and the 2(-Delta Delta C(T)) method. *Methods.* 25, 402-408. https://doi.org/10.1006/meth.2001.1262

Luyckx, M., Hausman, J.F., Lutts, S., Guerriero, G., 2017. Silicon and plants: current knowledge and technological perspectives. *Front. Plant Sci.* 8, 411. https://doi.org/10.3389/fpls.2017.00411

Ma, J.F., Yamaji, N., Mitani-Ueno, N., 2011. Transport of silicon from roots to panicles in plants. *Proc. Japan Acad., Ser B.* 87, 377-385 https://doi.org/10.2183/pjab.87.377

Maryani, N., Lombard, L., Poerba, Y.S., Subandiyah, S., Crous, P.W., Kema, G.H.J., 2019. Phylogeny and genetic diversity of the banana Fusarium wilt pathogen, in Indonesian center of origin. *Studies Mycol.* 92, 155- 194. https://doi.org/10.1016/j.simyco.2018.06.003

Müller, M., Munné-Bosch, S., 2015. Ethylene response factors: a key regulatory hub in hormone and stress signaling. *Plant Physiol.* 169, 32–41.

Pambudi, A., Maryanto, B.A., Effendi, Y., Sudirman, L.I., Miftahudin, M., 2023. Analysis of silicon-induced genes related to defense system in banana. *IOP Conf. Ser.: Earth Environ. Sci.* 1271, 012098. https://doi.org/10.1088/1755-1315/1271/1/012098

Peng, H., Feng, H., Zhang, T., Wang, Q., 2023. Editorial: plant defense mechanisms in plant-pathogen interactions. *Front. Plant Sci.* 14, 1292294. https://doi.org/10.3389/fpls.2023.1292294

Pieterse, C.M.J., Zamioudis, C., Berendsen, R.L, Weller, D.M., van Wees, S.C.M., Bakker, P.A.H.M., 2014. Induced systemic resistance by beneficial microbes. *Annu Rev Phytopathol.* 52, 347–375. https://doi.org/10.1146/annurev-phyto-082712-102340

Putri, R.E., Mubarik, N.R., Ambarsari, L., Wahyudi, A.T., 2023. Antifungal substances produced by *B. subtilis* strain W3.15 inhibit the *F. oxysporum* and trigger cellular damage. *Hayati J. Biosci.* 30, 843-854. https://doi.org/10.4308/hjb.30.5.843-854

Rodrigues, F.A., Resende, R.S., Dallagnol, L.J., Datnoff, L.E., 2015. *Silicon Potentiates Host Defense Mechanisms Against Infection by Plant Pathogens,* in: Rodrigues, F., Datnoff, L. (Eds.), *Silicon and Plant Diseases.* Springer, Cham, pp. 109–138. https://doi.org/10.1007/978-3-319-22930-0_5

Sun, S., Yang, Z., Song, Z., Wang, N., Guo, N., Niu, J., Liu, A., Bai, B., Ahammed, G.J., Chen, S., 2022. Silicon enhances plant resistance to Fusarium wilt by promoting antioxidant potential and photosynthetic capacity in cucumber (*Cucumis sativus* L.). *Front. Plant. Sci.* 13, 1011859. https://doi.org/10.3389/fpls.2022.1011859

van Bockhaven, J., de Vleesschauwer, D., Höfte, M., 2012. Towards establishing broad-spectrum disease resistance in plants: silicon leads the way. *J. Exp. Bot.* 64, 1281–1293. https://doi.org/10.1093/jxb/ers329

van Dongen, J.T., Licausi, F., 2015. Oxygen sensing and signaling. *Annu. Rev. Plant Biol.* 66, 345-67. https://doi.org/10.1146/annurev-arplant-043014-114813

Verma, K.K., Song, X.P., Liang, Q., Huang, H.R., Bhatt, R., Xu, L., Chen, G.L., Li, Y.R., 2024. Unlocking the role of silicon against biotic stress in plants. *Front. Plant Sci.* 15, 1430804. https://doi.org/10.3389/fpls.2024.1430804

Wang, M., Gao, L., Dong, S., Sun, Y., Shen, Q., Guo, S., 2017. Role of silicon on plant-pathogen interactions. *Front. Plant Sci.* 8, 701. https://doi.org/10.3389/fpls.2017.00701

Wu, Y., Li, X., Zhang, J., Zhao, H., Tan, S., Xu, W., Pan, J., Yang, F., Pi, E., 2022. ERF subfamily transcription factors and their function in plant responses to abiotic stresses. *Front Plant Sci.* 13, 1042084. https://doi.org/10.3389/fpls.2022.1042084

Xu, X., Chen, C., Fan, B., Chen, Z., 2006. Physical and functional interactions between pathogen-induced Arabidopsis WRKY18, WRKY40, and WRKY60 transcription factors. *Plant Cell.* 18, 1310-26. https://doi.org/10.1105/tpc.105.037523

Zhou, G.D., He, P., Tian, L., Xu, S., Yang, B., Liu, L., Wang, Y., Bai, T., Li, X., Li, S., Zheng, S.J., 2023. Disentangling the resistant mechanism of Fusarium wilt TR4 interactions with different cultivars and its elicitor application. *Front. Plant Sci.* 14, 1145837. https://doi.org/10.3389/fpls.2023.1145837